Excitation of the low-energy ^{229m}Th isomer in the electron bridge process via the continuum

P. V. Borisyuk,[1] N. N. Kolachevsky,[2,1,3] A. V. Taichenachev,[4,5] E. V. Tkalya,[2,1,6,*] I. Yu. Tolstikhina,[2] and V. I. Yudin[4,5,7,†]

[1]*National Research Nuclear University MEPhI, 115409, Kashirskoe shosse 31, Moscow, Russia*

[2]*P.N. Lebedev Physical Institute of the Russian Academy of Sciences, 119991, 53 Leninskiy Prospekt, Moscow, Russia*

[3]*Russian Quantum Center, 143025 Skolkovo, Moscow, Russia*

[4]*Novosibirsk State University, 2 Pirogova St., Novosibirsk, 630090, Russia*

[5]*Institute of Laser Physics SB RAS, Prospekt Akademika Lavrent'eva 13/3, Novosibirsk, 630090, Russia*

[6]*Nuclear Safety Institute of RAS, Bol'shaya Tulskaya 52, Moscow 115191, Russia*

[7]*Novosibirsk State Technical University, Prospekt Karla Marksa 20, Novosibirsk, 630073, Russia*

(Received 8 July 2019; published 10 October 2019)

The paper studies the excitation of the ^{229}Th nucleus to the anomalously low-lying isomeric state $3/2^+(8.28 \pm 0.17$ eV) in the electron bridge process via the continuum of the electron spectrum. Resonant excitation of the nucleus was found to be always possible in the scheme, no matter where the electron levels of an atom or ion were located. Formulas for the excitation cross section by narrow and wide laser lines are obtained. In the resonance, where the process under consideration turns into laser photoionization followed by nuclear excitation in electron capture, the cross section of the process was shown to be comparable in magnitude with that of the photoionization of the thorium atom. Experimental schemes for testing the effect were proposed, which would allow measuring the frequency of the nuclear isomeric transition $3/2^+ \to 5/2^+$ to a high precision, which is the first-priority (and still unresolved) task for creating a nuclear clock.

DOI: 10.1103/PhysRevC.100.044306

I. INTRODUCTION

An anomalously low-lying state of $E_{\rm is}$ energy in the range of 8.1–8.5 eV in the ^{229}Th nucleus [1] offers ambitious prospects for research in the convergence of low-energy nuclear physics with other fields of science, i.e., solid state physics, laser physics, plasma physics, optics, and others. References to the potential existence of a low-lying level $3/2^+(E_{\rm is} < 100$ eV) in ^{229}Th were first made in the work [2]. However, thanks to works [3,4] it turned out that in this case we were dealing with the transition of optical energy. According to 2007 measurements, the level energy is 7.6 ± 0.5 eV [5,6]. The most recent isomer energy data are given in [1]. According to them, $E_{\rm is} = 8.28 \pm 0.17$ eV.

Nowadays, characteristics of isomeric state $3/2^+(8.28 \pm 0.17$ eV) and parameters of the $M1$ nuclear transition from isomeric to the ground state $5/2^+(0.0)$ are being actively explored. Works [1,7,8] have revealed an internal conversion (IC), which is direct evidence of a low-lying level, and primarily estimated its lifetime. The magnetic dipole and electric quadrupole moments of the isomeric level were measured in [9], and the charge radius of the ^{229m}Th nucleus was found in [10].

A great interest in this unique nuclear state is determined by a number of new fundamental physical effects and promising applications which could be realized with the help of ^{229m}Th. Among the most notable ones is a "nuclear clock" [11–14], a nuclear laser in the optical range [15,16], tests of the variation of strong interaction parameter [17–20] and the fine structure constant [21], controlling γ decay via boundary conditions (the Purcell effect) [22], the α decay of the isomeric state [23], the Mössbauer effect in the optical range [15], and others.

The effective excitation of ^{229}Th nuclei to the given isomeric state is one of the most significant challenges. It should significantly speed up the exploration of the above phenomena. With the energy of an isomeric nuclear transition lying in the optical region of the spectrum, intense laser radiation could be used to excite ^{229}Th [24]. Meanwhile, there are two excitation channels of the isomeric state: direct photoexcitation with the direct absorption of resonance photons by the nuclei [24], and the so-called electron bridge (EB) [24–26], a third-order process for the electromagnetic interaction constant e, where the electron shell serves as an intermediate link between laser photons and the nucleus.

The concept of an electron bridge was introduced into physics by Krutov (see [27] and references therein). In works [28,29] it was used to describe the $E3$ (76 eV) nuclear transition in ^{235}U between the ground state and the first excited state. Decay of a low-lying isomer in ^{229}Th over the electron bridge channel was first studied in [30]. The inverse process—the excitation of nuclei in the process of the electron bridge through discrete and continuous parts of the electron spectrum—was first considered in [31] for ^{235}U. In works [25,26,32], the electron bridge was proposed to excite the ^{229m}Th isomer. Since at that time the value of

*tkalya_e@lebedev.ru

†viyudin@mail.ru

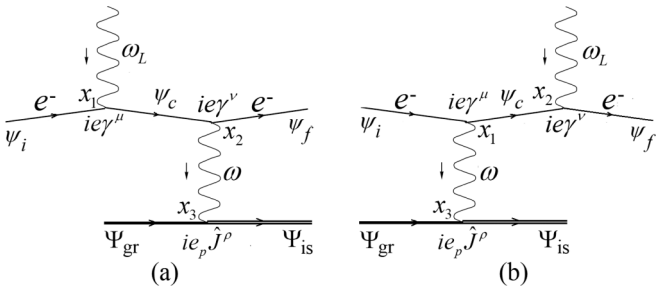

FIG. 1. Direct (a) and exchange (b) Feynman diagrams of the EB process.

$E_{is} = 1 \pm 4$ eV [3] was taken for the isomer energy, with the ionization potential of the thorium atom being equal to 6.3 eV, the case of excitation was studied only via the discrete spectrum. Subsequently, the electron bridge to excite the ^{229}Th nucleus in thorium ions was discussed in [33,34], and others.

In this paper, we consider the excitation of the $3/2^+(8.28 \pm 0.17$ eV) isomeric level in ^{229}Th by the electron bridge mechanism via the continuous part of the electron spectrum, and show that in some cases the process can have cross sections which are sufficient enough for the isomer to be effectively excited. On the basis of the results, we propose an experimental scheme on the photoionization of ^{229}Th neutral atoms. The experiment will allow us to determine the frequency of the $M1$ nuclear transition between the low-lying isomeric and the ground states $5/2^+ \to 3/2^+$ to a high precision, which is sufficiently enough to put the "nuclear clock" in practice.

II. THEORY OF THE ELECTRON BRIDGE

The nucleus excitation in the electron bridge process is described by two third-order Feynman diagrams (see Fig. 1). These diagrams correspond to a third-order S-matrix element [35]

$$S_{fi}^{(3)} = \int d^4x_1 d^4x_2 d^4x_3\, \bar{\psi}_f(x_2) ie\gamma^\nu G(x_2, x_1) ie\gamma^\mu \psi_i(x_1) \times [A_\mu(x_1) D_{\nu\rho}(x_3 - x_2) + A_\nu(x_2) D_{\mu\rho}(x_3 - x_1)] \times \Psi_{is}^+(x_3) ie_p \hat{J}^\rho \Psi_{gr}(x_3), \quad (1)$$

where e and e_p are electron and proton charges, correspondingly, $\hat{J}^\rho$ is the nuclear current operator, $x_j = (t_j, \mathbf{r}_j)$ for $j = 1, 2, 3$ are the vertex coordinates, and γ^μ are the Dirac matrices.

Let us take a photon wave function in the form

$$A_\mu(x) = e^{-i\omega_L t} A_\mu(\mathbf{r}),$$

where ω_L is the laser photon energy. Photon propagators in the diagrams in Fig. 1 are written down as Fourier transforms of the propagation functions in the frequency-coordinate representation (that is, through integrals over the energy of the virtual photon)

$$D_{\mu\rho}(x_i - x_j) = \int \frac{d\omega}{2\pi} e^{-i\omega(t_i - t_j)} D_{\mu\rho}(\omega; \mathbf{r}_i - \mathbf{r}_j).$$

The electron propagator (Green's function) in (1) is generally written down as a sum over discrete (bound) states with negative energy $E_n < 0$ and integral over states of the continuum spectrum with positive energy $E_c > 0$,

$$G(x_2, x_1) = \sum_n \psi_n(x_2)\, \bar{\psi}_n(x_1) + \int \psi_c(x_2)\, \bar{\psi}_c(x_1) \frac{d^3 p_c}{(2\pi)^3}.$$

As stated above, excitation of the nucleus via bound states is described in detail in many works [25,26,32–34]. Therefore, we shall limit ourselves here to considering the process through a continuous part of the spectrum. Note that the inverse process, namely, the decay of the isomer ^{229m}Th via the electron bridge, taking into account the states of the electron continuum, has already been considered in different approaches and with varying degrees of detail in [36–39]. Here we give a sequential derivation of formulas for the cross section of the ^{229}Th nucleus excitation process in the framework of perturbation theory for quantum electrodynamics.

Wave functions (WFs) of an electron in the initial $|i\rangle$ of the E_i energy, the final $|f\rangle$ of the E_f energy and intermediate $|c\rangle$ of the E_c energy states are

$$\psi_{i(f,c)}(x) = e^{-iE_{i(f,c)}t} \psi_{i(f,c)}(\mathbf{r}),$$

and wave functions of the nucleus in the ground state of the E_{gr} energy and isomeric state of the E_{is} energy are

$$\Psi_{gr}(x) = e^{-iE_{gr}t} \Psi_{gr}(\mathbf{r}),$$
$$\Psi_{is}(x) = e^{-i(E_{is} - i\Gamma_{is}^{tot}/2)t} \Psi_{is}(\mathbf{r}).$$

Moreover, we introduced a full width of nuclear level Γ_{is}^{tot} into the WF of the final (isomeric) state of the nucleus (the system of units $\hbar = c = 1$ is used).

Now the S-matrix element (1) takes the form

$$S_{fi}^{(3)} = \int dt_1 dt_2 dt_3 \int d^3r_1 d^3r_2 d^3r_3 \int \frac{d^3p_c}{(2\pi)^3} \int \frac{d\omega}{2\pi} \times e^{iE_f t_2} \bar{\psi}_f(\mathbf{r}_2) ie\gamma^\nu e^{-iE_c t_2} \psi_c(\mathbf{r}_2) \times \bar{\psi}_c(\mathbf{r}_1) e^{iE_c t_1} ie\gamma^\mu e^{-iE_i t_1} \psi_i(\mathbf{r}_1) \times [e^{-i\omega_L t_1} A_\mu(\mathbf{r}_1) e^{i\omega(t_3 - t_2)} D_{\nu\rho}(\omega; \mathbf{r}_3 - \mathbf{r}_2) + e^{-i\omega_L t_2} A_\nu(\mathbf{r}_2) e^{i\omega(t_3 - t_1)} D_{\mu\rho}(\omega; \mathbf{r}_3 - \mathbf{r}_1)] \times e^{i(E_{is} - i\Gamma_{is}^{tot}/2)t_3} \Psi_{is}^+(\mathbf{r}_3) ie_p \hat{J}^\rho \Psi_{gr}(\mathbf{r}_3) e^{-iE_{gr}t_3}. \quad (2)$$

Time integration in expression (2) is carried out using the integral representation of the delta function

$$\delta(\Omega) = \frac{1}{2\pi} \int e^{i\Omega t} dt \quad (3)$$

and the formula

$$\int e^{i(\varepsilon + i\Gamma/2)t} dt = \frac{i}{\varepsilon + i\Gamma/2}, \quad (4)$$

which follows from the expression which is readily provable by the residue theory

$$e^{i(\varepsilon + i\Gamma/2)t} = \frac{1}{2\pi i} \int \frac{e^{i\varepsilon t} dE}{E - (\varepsilon + i\Gamma/2)}.$$

Substituting (3) and (4) into (2) and integrating over times t_1, t_2, t_3, we have for the direct (a) and exchange (b) diagrams in Fig. 1, correspondingly,

$$2\pi\delta(E_f - E_c - \omega)\,2\pi\delta(E_c - E_i - \omega_L)\frac{i}{\omega_N + \omega + i\Gamma_{\rm is}^{\rm tot}/2},$$

$$2\pi\delta(E_f - E_c - \omega_L)\,2\pi\delta(E_c - E_i - \omega)\frac{i}{\omega_N + \omega + i\Gamma_{\rm is}^{\rm tot}/2}.$$

Now we involve the notation ω_N for the energy of nuclear transition $\omega_N = E_{\rm is} - E_{\rm gr}$.

Subsequently integrating over ω and $\mathbf{p}_c$ ($d^3p_c = mp_c dE_c d\Omega_{\mathbf{p}_c}$, $E_c = p_c^2/2m$ is the kinetic energy, and m is the electron mass) we have

$$\begin{aligned} S_{fi}^{(3)} = {} & \frac{i}{E_f + \omega_N - \omega_L - E_i + i\Gamma_{\rm is}^{\rm tot}/2}\frac{mp_c}{\pi} \\ & \times \int d^3r_1 d^3r_2 d^3r_3 \bar{\psi}_f(\mathbf{r}_2) ie\gamma^\nu \\ & \times [\psi_{E_c=E_i+\omega_L}(\mathbf{r}_2)\bar{\psi}_{E_c=E_i+\omega_L}(\mathbf{r}_1) \\ & \times A_\mu(\mathbf{r}_1) D_{\nu\rho}(\omega; \mathbf{r}_3 - \mathbf{r}_2) \\ & - \psi_{E_c=E_i-\omega_N}(\mathbf{r}_2)\bar{\psi}_{E_c=E_i-\omega_N}(\mathbf{r}_1) \\ & \times A_\nu(\mathbf{r}_2) D_{\mu\rho}(\omega; \mathbf{r}_3 - \mathbf{r}_1)] ie\gamma^\mu \psi_i(\mathbf{r}_1) \\ & \times \Psi_{\rm is}{}^+(\mathbf{r}_3) ie_p \hat{J}^\rho \Psi_{\rm gr}(\mathbf{r}_3). \end{aligned}$$

In the direct diagram, the intermediate states ψ_c lie in the positive energy region $E_c = E_i + \omega_L$, while in the exchange diagram they have negative energies $E_c = E_i - \omega_N < 0$. This will allow omitting the exchange diagram and operating only the direct one. As discussed later, this fact simplifies the calculation drastically and leads to the factorization of the third-order process by the product of the first- and second-order processes.

The cross section for the S-matrix element is obtained from the formula [35]

$$\sigma_{\rm EB}(\omega_L) = \frac{1}{2j_i+1}\frac{1}{2I_{\rm gr}+1}\frac{1}{2}\sum_{\substack{m_i,m_f \\ M_{\rm gr},M_{\rm is} \\ \kappa}} \frac{\left|S_{fi}^{(3)}\right|^2}{T}. \tag{5}$$

Summing in (5) is carried out by magnetic quantum numbers of electron m_i, m_f, and nucleus $M_{\rm gr}$, $M_{\rm is}$, and photon polarizations κ, j_i and $I_{\rm gr}$ are respectively the electron and the nucleus spin in the initial state. The characteristic time of the process is $T \simeq 1/\Gamma_{\rm is}^{\rm tot}$. As a result, we have for the cross section

$$\begin{aligned} \sigma_{\rm EB}(\omega_L) = {} & \frac{\Gamma_{is}^{\rm tot}}{(E_f + \omega_N - E_i - \omega_L)^2 + \left(\Gamma_{\rm is}^{\rm tot}/2\right)^2} \\ & \times \frac{1}{2j_i+1}\frac{1}{2I_{gr}+1}\frac{1}{2}\left(\frac{mp_c}{\pi}\right)^2 \sum_{\substack{m_i,m_f \\ M_{gr},M_{\rm is} \\ \kappa}} \\ & \times \left|\int d^3r_1 \bar{\psi}_c(r_1) ie\gamma^\mu \psi_i(\mathbf{r}_1) A_\mu(\omega_L, \mathbf{r}_1)\right|^2 \\ & \times \left| \int d^3r_2 d^3r_3 \bar{\psi}_f(\mathbf{r}_2) ie\gamma^\nu \psi_c(\mathbf{r}_2) \right. \\ & \left. \times D_{\nu\rho}(\omega_N; \mathbf{r}_3 - \mathbf{r}_2)\Psi_{\rm is}^+(\mathbf{r}_3) ie_p \hat{J}^\rho \Psi_{\rm gr}(\mathbf{r}_3)\right|^2, \end{aligned} \tag{6}$$

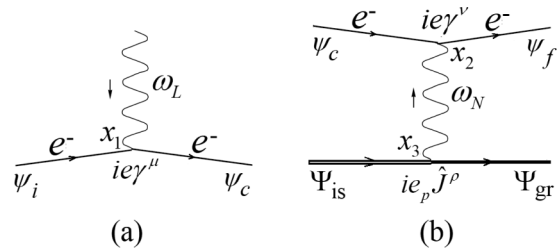

FIG. 2. Feynman diagrams of photoionization (a) and internal conversion (b).

where only those intermediate states are considered for which $E_c = E_i + \omega_L$.

In (6), the EB factorization can be clearly seen. In the resonance, where the continuum state plays the role of a real state, the intermediate-state electron line is cut between points x_1 and x_2 in the direct diagram in Fig. 1(a). In this case the EB process would split into the ionization of atomic shell $|i\rangle$, with the electron emitting into the continuum state $|c\rangle$, and the nucleus excitation in the electron capture from the continuum $|c\rangle$ to the final (bound) electron state in the atom $|f\rangle$.

The process of nuclear excitation during the capture of a free electron into a bound state of the ion was proposed by Goldanskii and Namiot in 1976 [40]. The authors named it inverse internal electron conversion (IIEC), since this process essentially is inverse to the internal electron conversion, the well-known decay channel of the isomeric nuclear state, when the excitation energy transfers to one of atomic electrons, resulting in ionization of the atom. However, currently, in publications, this process is referred to as nuclear excitation by electron capture (NEEC). Using this terminology, the resonant excitation of the nucleus via the electron shell can be called laser-photoionization followed by NEEC. (Note that the NEEC process should not be confused with the *electroweak* process of nuclear excitation by electron capture, i.e., the process in which the nucleus excites when it absorbs an atomic shell electron in the reaction $p + e^- \to n + \nu_e$.)

In view of the foregoing, we can rewrite formula (6) more clearly. Let us find expressions for the photoionization cross section of the electron shell $|i\rangle$ as shown in Fig. 2(a), and internal electron conversion from the shell as shown in Fig. 2(b).

In taking the first-order S-matrix element which corresponds to the diagram in Fig. 2(a)

$$S_{ic}^{(1)} = \int \bar{\psi}_c(x_1) ie\gamma^\mu \psi_i(x_1) A_\mu(\omega_L, x_1) d^4x_1$$

and operating with it as detailed above for $S_{fi}^{(3)}$, we obtain the following expression for the photoionization cross section:

$$\begin{aligned} \sigma_{\rm ion}(\omega_L) = {} & \frac{1}{2j_i+1}\frac{1}{2}\frac{mp_c}{\pi}\sum_{\substack{m_i,m_c \\ \kappa}} \left| \int d^3r_1 \right. \\ & \left. \times \bar{\psi}_c(\mathbf{r}_1) ie\gamma^\mu \psi_i(\mathbf{r}_1) A_\mu(\omega_L, \mathbf{r}_1)\right|^2, \end{aligned} \tag{7}$$

where $E_c = E_i + \omega_L$ as mentioned above.

On performing similar operations on the second-order S-matrix element which describes internal electron conversion

$$S_{fc}^{(2)} = \int \bar{\psi}_c(x_2) ie\gamma^\nu \psi_f(x_2) D_{\nu\rho}(\omega; x_3 - x_2) \times \Psi_{\rm gr}^{+}(x_3) ie_p \hat{f}^\rho \Psi_{\rm is}(x_3) d^4x_2 d^4x_3,$$

the probability of IC during the electron transition from the bound state $|f\rangle$ to the continuum spectrum $|c\rangle$ as a result of nuclear transition with energy ω_N from the isomeric state $\Psi_{\rm is}$ to the ground state $\Psi_{\rm gr}$ will be expressed as

$$\Gamma_{\rm is}^{\rm IC}(\omega_N; f) = \frac{1}{2j_f+1}\frac{1}{2I_{\rm is}+1}\frac{mp_c}{\pi}\sum_{\substack{m_c,m_f\\ M_{\rm is},M_{\rm gr}}}\left|\int d^3r_2 d^3r_3 \times \bar{\psi}_c(\mathbf{r}_2) ie\gamma^\nu \psi_f(\mathbf{r}_2) D_{\nu\rho}(\omega_N; \mathbf{r}_3 - \mathbf{r}_2) \times \Psi_{\rm gr}^{+}(\mathbf{r}_3) ie_p \hat{f}^\rho \Psi_{\rm is}(\mathbf{r}_3)\right|^2. \quad (8)$$

Using expressions (7) and (8), we write the EB process cross section as

$$\sigma_{\rm EB}(\omega_L) = g\frac{\Gamma_{\rm is}^{\rm tot}\,\Gamma_{\rm is}^{\rm IC}(\omega_{\rm IC}; f)}{\left(\omega_L - \omega_L^{\rm res}\right)^2 + (\Gamma_{\rm is}^{\rm tot}/2)^2}\sigma_{\rm ion}(\omega_L), \quad (9)$$

where $\Gamma_{\rm is}^{\rm IC}(\omega_{\rm IC}; f)$ is the partial width (probability) of the $M1$ internal conversion from the $|f\rangle$ shell of the thorium atom at the virtual photon energy $\omega_{\rm IC} = \omega_L + E_i - E_f$ (it does not coincide with the nuclear transition energy ω_N far-off resonance), $\sigma_{\rm ion}$ is the photoionization cross section from Eq. (7). The full width of low-lying isomer nuclear level in ^{229}Th, $\Gamma_{\rm is}^{\rm tot}$, is the sum of all partial widths, namely, radiation and IC widths from the $7s$ and $6d$ atomic shells participating in the internal conversion; $\omega_L^{\rm res} = E_f - E_i + \omega_N$ is the resonant energy of laser photons ω_L at which the resonant excitation of nucleus occurs; and g is the statistical factor of order 1

$$g = \frac{2j_f+1}{2j_c+1}\frac{2I_{\rm is}+1}{2I_{\rm gr}+1}\frac{1}{(2j_c+1)^2},$$

which connects the excitation processes of the nucleus $\Psi_{\rm gr} \to \Psi_{\rm is}$ when an electron passes from the continuum $|c\rangle$ to the $|f\rangle$ state, and the decay of the isomeric state $\Psi_{\rm is} \to \Psi_{\rm gr}$ through the channel of internal conversion with the electron emission from the $|f\rangle$ shell to the continuum $|c\rangle$. Factor $1/(2j_c+1)^2$ occurred due to the summation over the final states in the WF ψ_c in photoionization and internal conversion processes in Fig. 2. There is no similar summation in the EB process in Fig. 1, where WF ψ_c describes an intermediate electron state.

Formula (9) corresponds to the excitation cross section of the nucleus as having a very narrow laser beam, whose width is much shorter than the characteristic excitation widths of the involved atomic and nuclear states. It is possible that the laser line has a width which exceeds substantially the width of the nuclear level in (9). In order to account for that fact, we introduce the photon energy distribution function $g_L(\tilde{\omega} - \omega_L)$ normalized by the condition

$$\int g_L(\tilde{\omega} - \omega_L) d\tilde{\omega} = 1$$

and average the cross section (9) over it,

$$\sigma_{\rm EB}(\omega_L) = \int \sigma_{\rm EB}(\tilde{\omega})\, g_L(\tilde{\omega} - \omega_L) d\tilde{\omega}. \quad (10)$$

Let us choose a Lorentzian laser line, which is most frequent in the experiment,

$$g_L(\tilde{\omega} - \omega_L) = \frac{1}{2\pi}\frac{\Delta\omega_L}{(\tilde{\omega} - \omega_L)^2 + (\Delta\omega_L/2)^2}. \quad (11)$$

Integration over formula (10) with account of explicit form $\sigma_{\rm EB}$ from (9) and $g_L(\tilde{\omega} - \omega_L)$ from (11) leads to the expression for the EB cross section

$$\sigma_{\rm EB}(\omega_L) = g\frac{\Delta\omega_L\,\Gamma_{\rm is}^{\rm IC}(\omega_N; f)}{\left(\omega_L - \omega_L^{\rm res}\right)^2 + (\Delta\omega_L/2)^2}\sigma_{\rm ion}\left(\omega_L^{\rm res}\right), \quad (12)$$

which is valid at $\Gamma_{\rm is}^{\rm IC} \ll \Delta\omega_L$. For integration, we have made use of the fact that for small $\Gamma_{\rm is}^{\rm tot}$ and the condition $\Gamma_{\rm is}^{\rm tot} \ll \Delta\omega_L$, the following relation is satisfied:

$$\lim_{\Gamma_{\rm is}^{\rm tot}\to 0}\frac{1}{2\pi}\frac{\Gamma_{\rm is}^{\rm tot}}{\left(\tilde{\omega} - \omega_L^{\rm res}\right)^2 + \left(\Gamma_{\rm is}^{\rm tot}/2\right)^2} = \delta\left(\tilde{\omega} - \omega_L^{\rm res}\right).$$

In the resonance, as illustrated by the excitation scheme in Fig. 3, the EB cross section from the $|i\rangle$ shell to the $|f\rangle$ shell through the continuum can be written in an intuitively clear way:

$$\sigma_{\rm EB}\left(\omega_L^{\rm res}; i \to f\right) = g\frac{\Gamma_{\rm is}^{\rm IC}(\omega_N; f)}{\Delta\omega_L}\sigma_{\rm ion}\left(\omega_L^{\rm res}; i\right). \quad (13)$$

Far from resonance, there will be the $\Delta\omega_L\Gamma_{is}^{\rm IC}/(\omega_L - \omega_L^{\rm res})^2$ factor instead of the $\Gamma_{\rm is}^{\rm IC}/\Delta\omega_L$ factor in formula (13). It completely suppresses the excitation process of the nucleus if the detuning $\omega_L - \omega_L^{\rm res}$ significantly goes beyond the width of the laser line.

III. RESULTS AND DISCUSSION

The process considered in this paper has one principal advantage, namely, the resonant excitation of the nucleus via the electron continuum, whose schemes are shown in Fig. 3, is always available, regardless of the structure of atomic states or the magnitude of the energy of nuclear transition. This is not the case with the EB process via bound states. Here intermediate discrete levels have fixed, strictly defined energies E_n. For the nucleus to be effectively excited, there is a necessity for a resonant coincidence of energy $\omega_{nf} = E_f - E_n$ of atomic transition from the intermediate to the final state $|n\rangle \to |f\rangle$ with the nuclear transition energy ω_N. But it is still unknown whether such a pair of levels $|n\rangle$ and $|f\rangle$ exists in the atom or ion of thorium.

The same applies to cross sections. To estimate numerically the excitation cross section of the ^{229}Th nucleus by the EB mechanism through the continuum, there is no need to know the nuclear transition energy to the width of an intermediate atomic state ψ_n. In the continuum, there is always such a state ψ_c that the resonance condition $E_c - E_f = \omega_N$ is fulfilled. Therefore, we may give quite realistic estimates for $\sigma_{\rm EB}$ even now, when there is sufficiently large uncertainty in the energy of the isomer nuclear level.

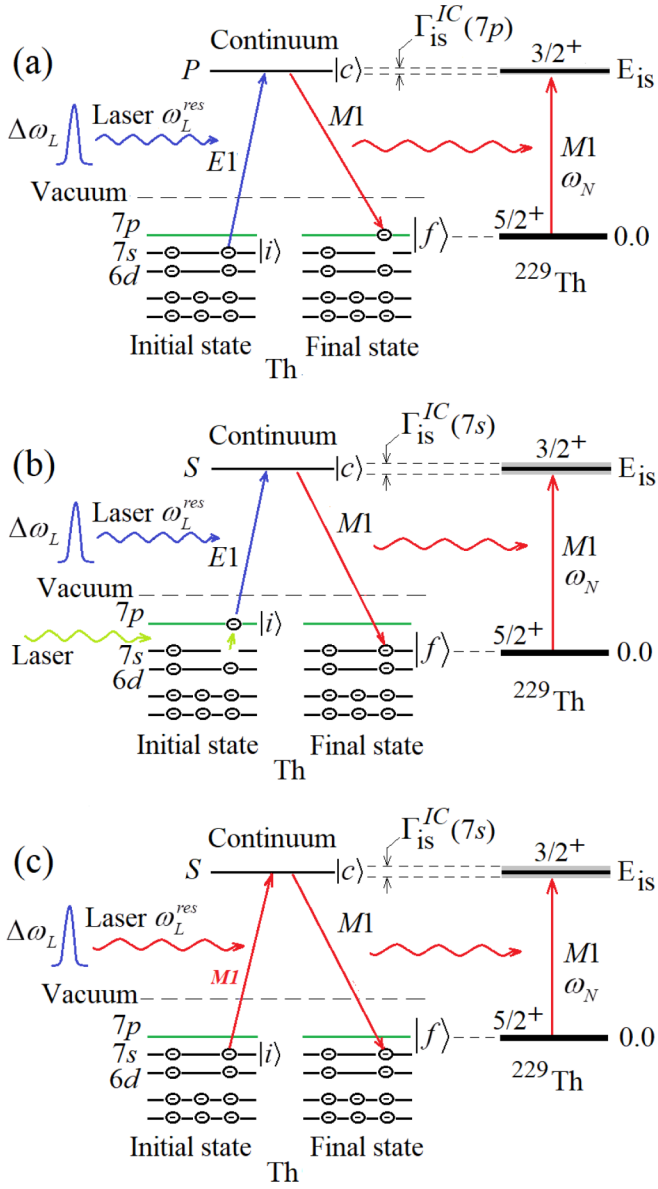

FIG. 3. ^{229m}Th excitation schemes in the EB process via continuum: (a) inelastic EB with the population of the excited atomic state; (b) inelastic EB with preliminary excitation of a Thorium atom; (c) elastic EB.

There are several approximately equivalent schemes for the effective excitation of the nucleus via the EB channel. First of all, it is an inelastic electron bridge, whose examples are given in Fig. 3(a) and 3(b). The initial $|i\rangle$ and final $|f\rangle$ states of the electron are different in an inelastic EB. In addition, the so-called multipole exchange is possible when the photon absorbed by the electron shell and the virtual photon exciting the nucleus in the second electron transition have different multipolarities. The nuclear isomeric transition in ^{229}Th is a magnetic dipole one. And the maximum contribution to the photoionization cross section is made by the $E1$ component of the plane wave. Therefore, the ^{229m}Th isomer excitation scheme with electronic transitions $|i\rangle \xrightarrow{E1} |c\rangle \xrightarrow{M1} |f\rangle$ is one of the most optimal ones.

TABLE I. Internal conversion widths $\Gamma_{is}^{IC}(\omega_N; f)$ of ^{229m}Th in units of $\Gamma_{is}^{IC}(\omega_N; 7s)$ for $\omega_N = 8.1$–8.5 eV.

$\|f\rangle$	$7s_{1/2}$	$6d_{3/2}$	$7p_{1/2}$	$8s_{1/2}$	$8p_{1/2}$	$9s_{1/2}$
$\Gamma_{is}^{IC}(f)/\Gamma_{is}^{IC}(7s)$	1	0.0025	0.023	0.078	0.0065	0.028

The choice of the final electron state $|f\rangle$ is also important. As can be seen from Table I, in the isomer decaying, the probability of internal conversion from the $7s$ atomic state significantly exceeds IC widths from the other levels. Accordingly, the working section of the laser photon spectrum, leading to the resonant excitation of the nucleus by the EB mechanism in the schemes in Figs. 3(b) and 3(c), where the final state is the $7s$ shell, is significantly larger than in the scheme in Fig. 3(a) with the $7p_{1/2}$ final state. In particular, for a similar reason, the process involving $6d$ electrons is less efficient, despite the fact that the cross section for photoionization of the $6d$ state is not inferior in magnitude to the cross section for photoionization of the $7s$ shell (see in Fig. 4).

When the initial and final states of the electron coincide, the ^{229}Th isomer can be excited by the elastic EB in electronic transitions as in $|i\rangle \xrightarrow{M1} |c\rangle \xrightarrow{M1} |f \equiv i\rangle$. According to Table I, probabilities of internal conversion from the $7s_{1/2}$ and $7p_{1/2}$ states satisfy the condition $\Gamma_{is}^{IC}(7p_{1/2}) \ll \Gamma_{is}^{IC}(7s_{1/2})$ and as we noted above, that fact has an impact on the magnitudes of the working sections of laser photon spectra. However, a major drawback of the scheme is that the partial cross section of photoionization $\sigma_{ion}(\omega_L; i \xrightarrow{M1} c)$ is smaller than the cross section $\sigma_{ion}(\omega_L; i \xrightarrow{E1} c)$ about eight orders of magnitude as was shown by the calculation using the FAC code (see the next paragraph). According to the scheme in Fig. 3(c), this makes an elastic EB for the ^{229}Th nucleus practically unobservable.

Let us estimate the EB cross section numerically. The photoionization cross sections are calculated using the FAC code

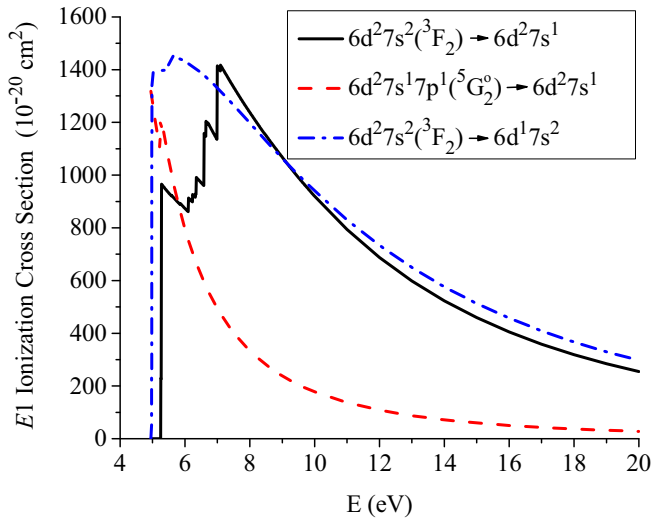

FIG. 4. Photoionization cross sections of the Th atom calculated using the FAC code (see the text).

based on the relativistic configuration interaction method [41]. Photoionization of the s electron ($E1$, $M1$) and d electron ($E1$) is calculated from the ground state of the Th atom $6d^2 7s^2$ ($^3F_2$), p electron from the $6d^2 7s7p$ ($^5G^o_2$) state with energy 1.793 eV (NIST database [42]; by comparison, FAC calculations give 1.759 eV). It can be seen that the partial cross sections of photoionization in Fig. 4 in the 8.1–8.5 eV photon energy range are approximately 10^{-17} cm^2.

When measured in [8], a half-life of the $3/2^+(8.28 \pm 0.17$ eV) state of the ^{229}Th nucleus $T_{1/2} = 7 \pm 1$ μs could be considered with the account of work [43] as a tentative value of a full conversion width of the level $\Gamma^{\rm tot}_{\rm is} \approx 10^{-10}$ eV.

If the width of the laser line satisfies the condition $\Gamma^{\rm tot}_{\rm is} \ll \Delta\omega_L$ and the formulas (12)–(13) are true, then the resonance cross section for the nucleus excitation in the EB process can be estimated from the relation $\sigma_{\rm EB} \sim 10^{-17} \times (10^{-10}/\Delta\omega_L)$, where $\Delta\omega_L$ is measured in electron-volts.

In irradiating the target by a laser with a very short width of line $\Delta\omega_L \ll \Gamma^{\rm IC}_{\rm is}(f)$ the formula (9) is valid. In this case, while selecting correctly the final state $|f\rangle$ the EB cross section in the resonance can practically be compared in magnitude with one of the partial photoionization cross sections in Fig. 4. As for the resonance photoexcitation cross section of the ^{229}Th nucleus, then it is calculated by the formula $\sigma_\gamma = (\lambda^2/2\pi)\Gamma^{\rm rad}_{\rm is}/\Delta\omega_L \simeq 3.6 \times 10^{-20}\Gamma^{\rm IC}_{\rm is}/\Delta\omega_L$, since the radiation width of the isomeric level is $\Gamma^{\rm rad}_{\rm is} = \Gamma^{\rm IC}_{\rm is}/\alpha$, and the internal conversion coefficient is $\alpha \approx 10^9$ for $\omega_N = 8.1$–8.5 eV. We see that for a laser beam with the width of $\Delta\omega_L = 10^{-11}$–$10^{-12}$ eV the cross section σ_γ can be less than $\sigma_{\rm EB}$ by two and one orders of magnitude respectively.

Being far-off resonance, the EB cross section is quickly suppressed by the energy denominator—the square of the detuning which is equal to the difference between the energy of the laser photons and their resonance value. Thus, it is possible to excite a nucleus in the inverse electron bridge process via a continuum only in a very narrow part of laser photon energies around the resonant frequencies. And it should be several resonant frequencies in accordance with the permissible selection rules for the final states $|f\rangle$.

In scanning the observed energy range with a tunable laser with a line width $\Gamma^{\rm tot}_{\rm is} \ll \Delta\omega_L$ in the photoionization current graph there will be narrow "dips" with resonant photon energies, with a width of $\Delta\omega_L$, when there occurs excitation of the ^{229}Th nucleus isomeric state along with atomic shell photoionization.

Based on the above analysis, we consider several photoionization schemes in more detail in another graphical representation (compared to the one in Fig. 3). These schemes would allow detecting the resonance at the ω_N frequency of the nuclear isomeric transition $3/2^+ \to 5/2^+$ and measuring its magnitude to a high precision, which is the priority task to develop a nuclear clock. If we start from the initial atomic-nuclear $7s(5/2^+)$ state and the final state is $7s(3/2^+)$, then the contribution of direct single-photon ionization via the $E1$ transitions in the EB is absent (since these two states have the same parity), and the desired resonance would not be practically observed. However, this problem is solved by using two-photon or two-laser (cascade) schemes. The

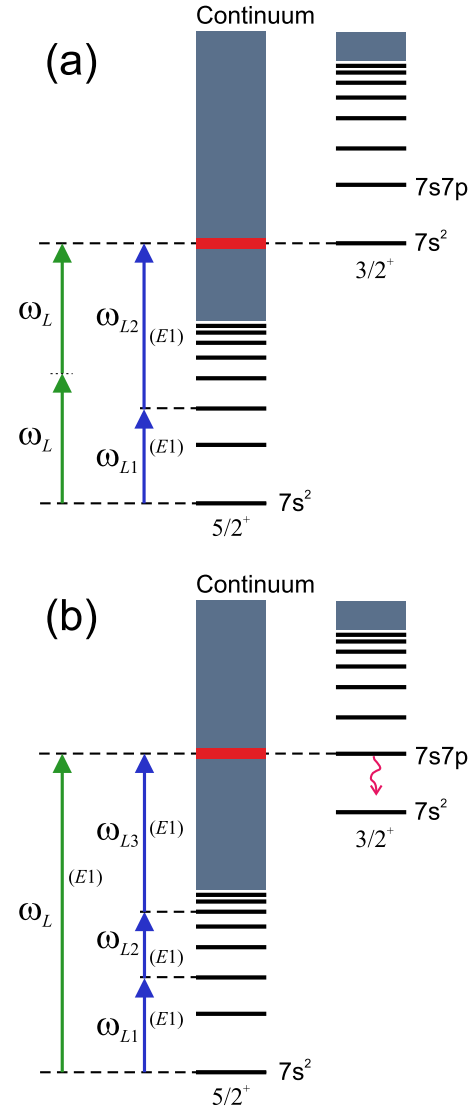

FIG. 5. Photoionization schemes to observe the EB resonance: (a) during internal conversion from the $7s(3/2^+)$ state; (b) during internal conversion from the $7p(3/2^+)$ state.

two-photon scheme is shown in Fig. 5(a) by green arrows. It describes the following case: the desired resonance is observed when the laser frequency ω_L is scanned near half the frequency of the nuclear isomeric transition $3/2^+ \to 5/2^+$. The cascade scheme shown by blue arrows in Fig. 5(a) may prove to be more efficient and flexible. Here, the lower laser with a fixed frequency ω_{L1} resonantly excites (akin to the $E1$ transition) some intermediate atomic level of the discrete spectrum, and the upper laser with a tunable frequency ω_{L2} performs photoionization. In this case, the desired resonance will be observed when the sum of frequencies $(\omega_{L1} + \omega_{L2})$ varies near the frequency of the nuclear isomeric transition $3/2^+ \to 5/2^+$. Similarly, a cascade scheme can be described using four (six and so on) lasers.

In our opinion, another promising alternative is when the initial state is $7s(5/2^+)$, and the final one is the p state of the electron in the external shell, for example, $7p(3/2^+)$

[see Figs. 5(b) and 3(a)]. In this case, parities of the initial and final states are different and, therefore, the EB process can be performed by the direct single-photon $E1$ ionization, which is shown in Fig. 5(b) by a green arrow, and the desired resonance will be observed at the frequency $\omega_L = (\omega_N + \omega_{s-p})$, where ω_{s-p} is a well-known frequency of the optical intra-atomic transition $7p \to 7s$. However, as the expected frequency of the isomeric transition $\omega_N = 8.1$–8.5 eV it is extremely difficult to find a laser source in that short-wave region. Therefore, one can use three-photon or cascade three-laser ionization shown by blue arrows in Fig. 5(b). In this cascade, two lower lasers with fixed frequencies ω_{L1} and ω_{L2} excite any two convenient (from a practical point of view) intra-atomic dipole transitions, and the frequency of the third laser ω_{L3} varies in the region of the resonance: $(\omega_{L1} + \omega_{L2} + \omega_{L3}) = (\omega_N + \omega_{s-p})$. Similarly, one can describe five-laser cascade ionization.

It is to be noted that since the probability of internal conversion from the $7s$ state of the atom significantly exceeds the internal conversion widths from other levels (and in particular from the $7p$ state), in terms of the resonances magnitude in the photoionization spectrum, the case shown in Fig. 5(a) is preferable to the diagram in Fig. 5(b). However, the case in Fig. 5(b) has additional features due to the fact that the bound upper level $7p(3/2^+)$ decays spontaneously and rapidly into a lower level $7s(3/2^+)$, generating spontaneous photons at the frequency of the $7p \to 7s$ intra-atomic transition [a red wavy line in Fig. 5(b)]. Now these photons can also be used to detect the desired resonance if we use photodetection equipment selectively tuned to a narrow spectral region with a well-known frequency of $7p \to 7s$ transition. At the same time, sensitivity of this method can be even higher in detecting the EB resonance than in detecting a photoionization signal. In fact, since spontaneous $7p \to 7s$ photons are entirely absent far-off resonance, the desired EB resonance will have a zero background, whose noise background will be determined only by the apparatus dark noise. Moreover, when using the photoionization signal, a narrow and small EB resonance will be observed against a large background with a fairly high noise level, which significantly reduces the signal-to-noise ratio.

It should be noted that the account of the fine and hyperfine structure will give nothing that is ground breaking. When measuring, instead of a single EB resonance, we will have several smaller and narrower ones.

In conclusion, we compare EB via the continuum and discrete parts of the electronic spectrum. In addition to the important features of both processes described at the very beginning of this section, we should note that the smallness of photoionization cross section can be considered as a relational disadvantage of EB via the continuum. The cross section of resonant photoexcitation of an atom $\sigma_{\rm exc}$, which is a component of the EB cross section through discrete levels $\sigma^{\rm d}_{\rm EB}$ [25,26]

$$\sigma^{\rm d}_{\rm EB} \simeq \sigma_{\rm exc} P_{\rm NEET},$$

is proportional to the square of the transition wavelength, i.e., relatively large. The photoionization cross section is much smaller. On the other hand, the relative probability of the nucleus excitation in the second (inverse) atomic transition between the bound states, $P_{\rm NEET}$, is included into the EB cross section via the discrete spectrum. The function $P_{\rm NEET}$ and the nuclear excitation in electron transition (NEET) process were suggested by Morita in 1973 [44]. As a rule, the value $P_{\rm NEET}$ is much smaller than unity [25,26,45] and depends on the structure of atomic wave functions. And in case of the EB cross section via the continuum, an additional reducing factor is either the ratio of the partial internal conversion width to the width of the laser line, or the ratio of the partial and total IC widths of the isomeric state. These two factors can be made close to unity by the appropriate choice of emitter, which compensates for the above-mentioned smallness of the photoionization cross section.

IV. CONCLUSION

In the paper we have studied the excitation of the low-lying isomer $3/2^+(8.28 \pm 0.17$ eV) of the ^{229}Th nucleus in the electron bridge process via continuum states. The given mechanism is shown to invariably provide resonant excitation of the nucleus, regardless of the structure and spectrum of atomic states. When the resonance occurs, this process can be seen as the laser photoionization followed by NEEC, which does not require any resonant coincidence between the energy of a nuclear transition and the energy of one of the atomic transitions between the bound states. It was found that when ^{229}Th atoms are under laser radiation with a very narrow line, the excitation cross section of the nucleus becomes comparable in magnitude to the partial photoionization cross section of the atomic electron shell. Altogether, this suggests that the EB process via the electron continuum should be a promising way of producing the isomeric nucleus ^{229m}Th. Based on the results, experimental schemes for testing the effect were proposed, which would allow measuring the frequency of nuclear isomeric transition $3/2^+ \to 5/2^+$ to a high precision, which is the first-priority (and still unresolved) task for creating a nuclear clock.

ACKNOWLEDGMENTS

This research was supported by a grant of the Russian Science Foundation (Project No. 19-72-30014). V.I.Y. was supported by the Ministry of Education and Science of the Russian Federation (Grant No. 3.1326.2017/4.6), and the Russian Foundation for Basic Research (Grant No. 17-02-00570). A.V.T. was supported by the Russian Foundation for Basic Research (Grant No. 18-02-00822).

[1] B. Seiferle, L. von der Wense, P. V. Bilous, I. Amersdorffer, C. Lemell, F. Libisch, S. Stellmer, T. Schumm, C. E. Dullmann, A. Palffy *et al.*, Nature **573**, 243 (2019).
[2] L. A. Kroger and C. W. Reich, Nucl. Phys. A **259**, 29 (1976).
[3] C. W. Reich and R. G. Helmer, Phys. Rev. Lett. **64**, 271 (1990).
[4] R. G. Helmer and C. W. Reich, Phys. Rev. C **49**, 1845 (1994).

[5] B. R. Beck, J. A. Becker, P. Beiersdorfer, G. V. Brown, K. J. Moody, J. B. Wilhelmy, F. S. Porter, C. A. Kilbourne, and R. L. Kelley, Phys. Rev. Lett. **98**, 142501 (2007).
[6] B. R. Beck, J. A. Becker, P. Beiersdorfer, G. V. Brown, K. J. Moody, J. B. Wilhelmy, F. S. Porter, C. A. Kilbourne and R. L. Kelley, Report LLNL-PROC-415170 (2009).
[7] L. von der Wense, B. Seiferle, M. Laatiaoui, J. B. Neumayr, H. J. Maier, H. F. Wirth, C. Mokry, J. Runke, K. Eberhardt, C. E. Dullmann *et al.*, Nature **533**, 47 (2016).
[8] B. Seiferle, L. von der Wense, and P. G. Thirolf, Phys. Rev. Lett. **118**, 042501 (2017).
[9] J. Thielking, M. V. Okhapkin, P. Glowacki, D. M. Meier, L. von der Wense, B. Seiferle, C. E. Dullmann, P. G. Thirolf, and E. Peik, Nature **556**, 321 (2018).
[10] M. S. Safronova, S. G. Porsev, M. G. Kozlov, J. Thielking, M. V. Okhapkin, P. Glowacki, D. M. Meier, and E. Peik, Phys. Rev. Lett. **121**, 213001 (2018).
[11] E. Peik and C. Tamm, Europhys. Lett. **61**, 181 (2000).
[12] W. G. Rellergert, D. DeMille, R. R. Greco, M. P. Hehlen, J. R. Torgerson, and E. R. Hudson, Phys. Rev. Lett. **104**, 200802 (2010).
[13] C. J. Campbell, A. G. Radnaev, A. Kuzmich, V. A. Dzuba, V. V. Flambaum, and A. Derevianko, Phys. Rev. Lett. **108**, 120802 (2012).
[14] E. Peik and M. Okhapkin, C. R. Phys. **16**, 516 (2015).
[15] E. V. Tkalya, Phys. Rev. Lett. **106**, 162501 (2011).
[16] E. V. Tkalya and L. P. Yatsenko, Laser Phys. Lett. **10**, 105808 (2013).
[17] V. V. Flambaum, Phys. Rev. Lett. **97**, 092502 (2006).
[18] H.-t. He and Z.-z. Ren, J. Phys. G: Nucl. Phys. **34**, 1611 (2007).
[19] A. Hayes and J. Friar, Phys. Lett. B **650**, 229 (2007).
[20] E. Litvinova, H. Feldmeier, J. Dobaczewski, and V. Flambaum, Phys. Rev. C **79**, 064303 (2009).
[21] J. C. Berengut, V. A. Dzuba, V. V. Flambaum, and S. G. Porsev, Phys. Rev. Lett. **102**, 210801 (2009).
[22] E. V. Tkalya, Phys. Rev. Lett. **120**, 122501 (2018).
[23] A. M. Dykhne, N. V. Eremin, and E. V. Tkalya, JETP Lett. **64**, 345 (1996).
[24] E. V. Tkalya, V. O. Varlamov, V. V. Lomonosov, and S. A. Nikulin, Phys. Scr. **53**, 296 (1996).
[25] E. V. Tkalya, JETP Lett. **55**, 211 (1992).
[26] E. V. Tkalya, Sov. J. Nucl. Phys. **55**, 1611 (1992).
[27] V. A. Krutov and V. N. Fomenko, Ann. Phys. **21**, 291 (1968).
[28] D. Hinneburg, M. Nagel, and G. Brunner, Z. Phys. A **291**, 113 (1979).
[29] D. Hinneburg, Z. Phys. A **300**, 129 (1981).
[30] V. F. Strizhov and E. V. Tkalya, Sov. Phys. JETP **72**, 387 (1991).
[31] E. V. Tkalya, Sov. Phys. Dokl. **35**, 1069 (1990).
[32] P. Kalman and T. Keszthelyi, Phys. Rev. C **49**, 324 (1994).
[33] S. G. Porsev, V. V. Flambaum, E. Peik, and C. Tamm, Phys. Rev. Lett. **105**, 182501 (2010).
[34] S. G. Porsev and V. V. Flambaum, Phys. Rev. A **81**, 042516 (2010).
[35] V. B. Berestetskii, E. M. Lifschitz, and L. P. Pitaevskii, *Quantum Electrodynamics* (Pergamon, Oxford, 1982).
[36] S. G. Porsev and V. V. Flambaum, Phys. Rev. A **81**, 032504 (2010).
[37] P. V. Bilous, E. Peik, and A. Palffy, New J. Phys. **20**, 013016 (2018).
[38] P. V. Bilous, Ph.D. thesis, Ruperto-Carola-University of Heidelberg, 2018.
[39] A. V. Andreev, A. B. Savel'ev, S. Y. Stremoukhov, and O. A. Shoutova, Phys. Rev. A **99**, 013422 (2019).
[40] V. I. Goldanskii and V. A. Namiot, Phys. Lett. B **62**, 393 (1976).
[41] M. F. Gu, Can. J. Phys. **86**, 675 (2008).
[42] A. Kramida, Yu. Ralchenko, J. Reader, and NIST ASD Team, NIST Atomic Spectra Database (ver. 5.6.1) [Online]. Available: https://physics.nist.gov/asd [2018, December 20] National Institute of Standards and Technology, Gaithersburg, MD (2018).
[43] P. V. Borisyuk, U. N. Kurel'chuk, O. S. Vasil'ev, V. I. Troyan, Y. Y. Lebedinskii, and E. V. Tkalya, Quant. Electron. **48**, 460 (2018).
[44] M. Morita, Prog. Theor. Phys. **49**, 1574 (1973).
[45] E. V. Tkalya, Nucl. Phys. A **539**, 209 (1992).